A simulation framework for spectral X-Ray imaging : application to the quantification of iodine in a thorax phantom

Nicolas Ducros, Razmig Kéchichian, Sébastien Valette, Philippe Douek, Françoise Peyrin

A simulation framework for spectral X-Ray imaging : application to the quantification of iodine in a thorax phantom

N. Ducros[1*], R. Kéchichian[1], S. Valette[1], P. Douek[1], Françoise Peyrin[1]

[1] CREATIS, Villeurbanne, France.
[*] Corresponding author : nicolas.ducros@creatis.insa-lyon.fr

Abstract - Thanks to the recent development in spectral detectors, X-Ray spectral imaging has received increasing attention. This technique permits the quantification of the chemical components in an object. We present material decompositions obtained from realistic numerical simulations that account for the spectral response function of the detector.

Index Terms - ***Spectral X-ray imaging, color CT, material decomposition***

I. INTRODUCTION

Spectral X-ray imaging (SXRI) is raising increasing interest in radiology owing to the new clinically relevant contrasts it can deliver. Similarly to dual-energy X-ray imaging, material decomposition algorithms can be used in SXRI for the recovery of the constituent materials, e.g. soft tissue and bone [1]. The most promising capability of SXRI is often considered to be K-edge imaging that can quantitatively resolve heavy elements such as iodine, gold, bismuth, or gadolinium. When targeted contrast agents carry a payload with a K-edge element, SXRI allows for molecular imaging. It has been shown that the concentration of the constituents of the human body (e.g. bone, water, fat) can be recovered together with the concentration in contrast agents [2]. Prototypes of SXRI systems are already available for small animal imaging but not yet for clinical imaging. There are still some issues related to detectors, the exploitation of data, and the material decomposition schemes [3].

SXRI has emerged thanks to the development of a new generation of photon counting detectors with energy discrimination capabilities [4]. Spectral detectors can classify X-ray photons into different energy bins depending on their energy. Although detectors are expected to count photons within given energy bins, some photons may be recorded within a wrong energy bin. This phenomena can be modeled by the response function of the detector. Although the imaging capabilities of a SXRI system are closely related to the energy discrimination capabilities of the detector [5], the detector response function is rarely taken into account. In this paper, we present a simulation framework in SXRI taking into account the detector response and first results for the quantification of iodine in an anatomical phantom of the thorax.

II. DIRECT PROBLEM

Let consider an object inside the domain Ω and characterized at energy E by its attenuation coefficient $\mu(\mathbf{r}, E), \mathbf{r} \in \Omega$. The number of photons transmitted through the object is given by the line integral

$$n(E) = n_0(E) \exp\left(-\int_{\mathcal{L}} \mu(\mathbf{r}, E)\, \mathrm{d}\mathbf{r}\right) \qquad (1)$$

where n_0 is the number of input photons and $\mathcal{L}$ is the path of integration that depends on the acquisition geometry. Let $n(E)$ be the number of photons entering a detector pixel with energy E. The output signal s_i provided by the detector in the output energy bin $[\mathcal{E}_i, \mathcal{E}_{i+1}]$ may be modeled by

$$s_i = \iint_{[\mathcal{E}_i, \mathcal{E}_{i+1}]\times\mathbb{R}} d(\mathcal{E}, E)\, n(E)\, \mathrm{d}E\, \mathrm{d}\mathcal{E} \qquad (2)$$

where $d(\mathcal{E}, E)$ is a probability density function that accounts for the probability of a photon reaching the detector at energy E to be detected at energy $\mathcal{E}$.

The probability density function of a detector can be obtained experimentally by measuring the detected photons for various incoming monochromatic X-ray beams, which can be achieved at synchrotron sources It can also be obtained numerically by using Monte Carlo simulations that take into account the physics of the detectors.

III. INVERSE PROBLEM

The standard approach consists in decomposing the object onto a basis of two materials [1]. In this case, the attenuation of the object modeled as:

$$\mu(\mathbf{r}, E) = \rho_1(\mathbf{r})\tau_1(E) + \rho_2(\mathbf{r})\tau_2(E) \qquad (3)$$

where τ_m, $m \in \{1, 2\}$, is the mass attenuation ($\mathrm{cm}^2.\mathrm{g}^{-1}$) of the mth material and ρ_m is its density ($\mathrm{g.cm}^{-3}$). Inserting (3) in (1) and (2) yields the measured signals s_i as a function of the object composition:

$$s_i = \iint_{[\mathcal{E}_i, \mathcal{E}_{i+1}]\times\mathbb{R}} d(\mathcal{E}, E)\, n_0(E) \mathrm{e}^{-a_1\tau_1(E) - a_2\tau_2(E)}\, \mathrm{d}E\, \mathrm{d}\mathcal{E} \qquad (4)$$

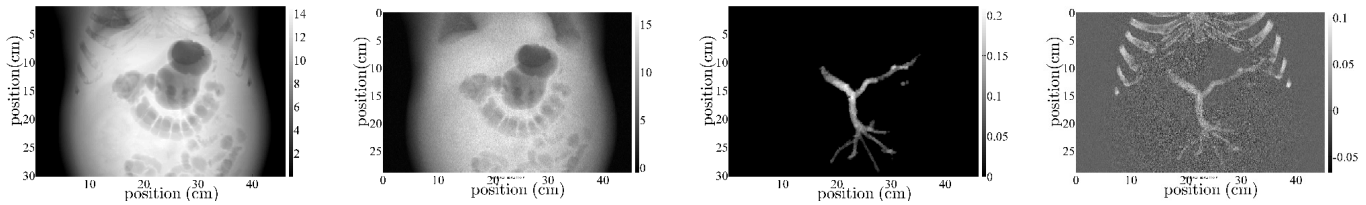

Figure 1: Material decomposition results. From top left to bottom right. a) Phantom soft-tissue, b) Decomposed soft-tissue , d) Phantom iodine, e) Decomposed iodine.

where

$$a_m = \int_{\mathcal{L}} \rho_m(\mathbf{r})\,\mathrm{d}\mathbf{r}, \quad \forall m \in \{1,2\} \tag{5}$$

is the area density (g.cm^{-2}) of material m along $\mathcal{L}$.

The material decomposition problem consists in finding the area density vector $\mathbf{a} = [a_1, \ldots, a_M]^\top$ from the measurement vector $\mathbf{s} = [s_1, \ldots, s_I]^\top$ knowing the mass attenuation vector $\boldsymbol{\tau}(E) = [\tau_1(E), \ldots, \tau_M(E)]^\top$.

The solution proposed by Alvarez and Macovski in [1] consists in assuming a polynomial relationship

$$\mathbf{a} = \mathcal{P}(\mathbf{s}) \tag{6}$$

where $\mathcal{P}$ is a second order polynomial and $\mathbf{s} = [s_1, \ldots s_I]^\top$ is the measurement vector. Then, the material decomposition problem is solved by a two-step algorithm.

- *Step 1: calibration of* $\mathcal{P}$. Measurements from known calibration phantoms are acquired. The polynomial coefficients are estimated by a least square approach. Let $\mathcal{P}^*$ denote the retained polynomial.

- *Step 2: decomposition*. The solution is readily given by

$$\mathbf{a}^* = \mathcal{P}^*(\mathbf{s}). \tag{7}$$

IV. RESULTS AND DISCUSSION

A spectral phantom requires the knowledge of the pair $\{\mathbf{a}, \boldsymbol{\tau}(E)\}$. Our phantom was built from the thorax phantom that was segmented in [6] using an approach based on clustering and graph cut. The linear attenuation of whether soft tissue or bone was attribute to each of the segments depending on its chemical nature. Then, the original CT volume was used to determine the local density. Finally, the portal vein was marked with iodine at a concentration of 0.1 g.cm^{-3}.

Material decomposition was performed by means of polynomial calibration. We considered the reconstruction of $M = 2$ materials, namely soft tissues and iodine, from $I = 2$ measurements. Measurements were corrupted with Poisson noise assuming 10^5 X-ray photons reached each pixel of the detector.

The phantom and decomposed area densities of soft tissues and iodine are represented at Fig. 1. The decomposed soft-tissue area density is in good agreement with the phantom soft-tissue area density (compare Fig. 1a and b)). The iodine decomposition nicely allows the portal vein to be identified. However, the bone tissue also appear, which can be improved considering a three-material decomposition at a higher cost of computational/time resource for the step 1 of polynomial calibration.

V. CONCLUSIONS

Our simulation framework for SXRI has been tested on a realistic anatomical phantom. In future work, we will consider three-material decomposition methods as well as more sophisticated inversion schemes including regularization. The methods are expected to be tested on experimental spectral data.

REFERENCES

[1] R E Alvarez and A Macovski. Energy-selective reconstructions in x-ray computerised tomography. *Physics in Medicine and Biology*, 21(5):733, 1976.

[2] C O Schirra, B Brendel, M A Anastasio, and E Roessl. Spectral CT: a technology primer for contrast agent development. *Contrast media & molecular imaging*, 9(1):62–70, February 2014.

[3] N G Anderson and A P Butler. Clinical applications of spectral molecular imaging: potential and challenges. *Contrast Media & Molecular Imaging*, 9(1):3–12, 2014.

[4] K Taguchi and J S Iwanczyk. Vision 20/20: Single photon counting x-ray detectors in medical imaging. *Medical Physics*, 40(10):100901, 2013.

[5] E. Roessl, B. Brendel, K. Engel, J. P Schlomka, A. Thran, and R. Proksa. Sensitivity of photon-counting based -edge imaging in x-ray computed tomography. *IEEE Transactions on Medical Imaging*, 30(9):1678–1690, 2011.

[6] R. Kechichian, S. Valette, M. Desvignes, and R. Prost. Shortest-path constraints for 3d multiobject semiautomatic segmentation via clustering and graph cut. *Image Processing, IEEE Transactions on*, 22(11):4224–4236, Nov 2013.